

Fig. 3. Output power and frequency variation as a function of varactor bias. Gunn device CXY 19/1-2. Varactor diode: *a*.

and the rectified RF current through the varactors was not more than 50  $\mu$ A. Following is a table of varactor diode parameters:

| Type     | $C_{j0}$<br>(pF) | $C_{j6}$<br>(pF) | $V_{BR}$<br>(V) | $V_P@1\text{ mA}$<br>(V) |
|----------|------------------|------------------|-----------------|--------------------------|
| <i>a</i> | 2.89             | 1.05             | 50              | 0.78                     |
| <i>b</i> | 1.67             | 0.59             | 50              | 0.76                     |
| <i>c</i> | 1.05             | 0.39             | 52              | 0.76                     |

The loaded  $Q$  of the cavities was estimated by frequency-pulling experiments. The variation in the values of  $Q_L$  was from 50 at zero varactor bias to 160 at -40 V varactor bias. These values for  $Q_L$  lie within the range obtainable in a single-post full-height waveguide cavity [4]. The FM noise of the oscillator of Fig. 2 *b* was measured and was found to be 65 rms Hz/ $\sqrt{\text{Hz}}$  at 1-KHz off-carrier. The oscillator frequency was 9.95 GHz.

It has been demonstrated that a wide-band varactor-tuned Gunn oscillator can be constructed in standard *X*-band waveguide cavity. Furthermore, the oscillator constructed in full-height waveguide shows less variation in the output power over the tuning range and eliminates the requirement for a transition to *X*-band waveguide. With a higher power Gunn device (CXY 19/1-2,  $P_0=170$  mW in test cavity) minimum power level of 90 mW with a variation of +1.3 dB and nearly 700 MHz of electronic tuning has been achieved (Fig. 3).

#### ACKNOWLEDGMENT

The author wishes to thank the members of the Semiconductor Measurements Laboratory for their help and co-operation, and J. A. F. Cornick for his continuous encouragement throughout this work.

#### REFERENCES

- [1] B. K. Lee and M. S. Hodgart, "Microwave Gunn oscillator tuned electronically over 1 GHz," *Electron. Lett.*, vol. 4, pp. 240-242, 1968.
- [2] R. B. Smith and P. W. Crane, "Varactor-tuned Gunn-effect oscillator," *Electron. Lett.*, vol. 6, pp. 139-140, 1970.
- [3] B. J. Downing and F. A. Myers, "Broadband (1.95 GHz) varactor-tuned *X* band Gunn oscillator," *Electron. Lett.*, vol. 7, pp. 407-409, 1971.
- [4] W. C. Tsai, F. J. Rosenbaum, and L. A. MacKenzie, "Circuit analysis of waveguide-cavity Gunn-effect oscillator," *IEEE Trans. Microwave Theory Tech. (Special Issue on Microwave Aspects of Avalanche-Diode and Transferred Electron Devices)*, vol. MTT-18, pp. 808-817, Nov. 1970.

#### Propagation Along Transversely Inhomogeneous Coaxial Transmission Lines

ROBERT E. MCINTOSH AND LUKE J. TURGEON

**Abstract**—Numerical "shooting" methods are employed in obtaining the dispersion curves of a coaxial waveguide loaded with a radially inhomogeneous dielectric. The utility of this technique is tested by comparing results with known analytical solutions. The method is also used to find the dispersion curves of a coaxial waveguide loaded with a radially Gaussian-distributed plasma.

#### I. INTRODUCTION

Propagation of electromagnetic (EM) signals along transversely inhomogeneous transmission lines is of current interest because of the potential that these lines show for various waveguide applications. Various treatments of circular transmission lines having a radial inhomogeneity of the permittivity have been previously reported. Ah Sam and Klinger [1], for example, obtained a dispersion relationship for a coaxial line where the dielectric constant is inversely proportional to the square of the radius. Yamada and Watanabe have solved the wave equation for the azimuthally symmetrical circular waveguide where the dielectric constant varies quadratically with the radius [2]. Unfortunately, analytical solutions of the transmission properties of radially inhomogeneous waveguides are unobtainable when the variation of the electrical properties of the medium is arbitrary. Much attention, therefore, has been given to numerical methods that employ finite-difference or variational techniques [3].

Numerical solutions have been obtained by various investigators for situations where the radially varying permittivity is approximated by a finite number  $N$  of concentric cylindrical shells [4], [5]. The dielectric constant of each of these shells is assumed to be constant, but not necessarily the same as the other shells. By assuming that the fields in each shell can be expressed in terms of Bessel functions, the problem is reduced to satisfying the boundary conditions at the inner

Manuscript received June 1, 1972; revised August 16, 1972. This work was supported in part by the Air Force Office of Scientific Research under Grant AFOSR G9-1722.

The authors are with the Department of Electrical Engineering, University of Massachusetts, Amherst, Mass. 01002.

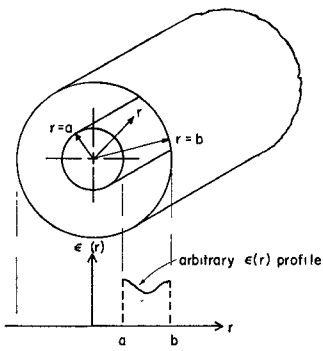


Fig. 1. Coaxial transmission system having an arbitrarily varying dielectric in the radial direction.

and outer surface of each shell. This is accomplished numerically by evaluating the eigenfrequencies of a system of  $4N-4$  simultaneous algebraic equations. The accuracy of this method improves, in principle, as the number of shells is increased. However, increased computing time and the accompanying machine errors offset this effect, particularly when the permittivity is strongly inhomogeneous or the radial variation of the fields is large, as in the case of higher order modes [4].

English [6] has successfully employed vector variational techniques in solving for EM wave transmission in a circular waveguide containing a concentric dielectric rod. This variational approach can be extended to the case where the radial variation of the dielectric medium is arbitrary. Although this approach should be advantageous in terms of reducing the computer storage requirements, some effort is needed in choosing trial fields that satisfy as many boundary conditions as possible.

In this short paper, we show that it is advantageous in the case of a transversely inhomogeneous coaxial line to numerically solve for each of the field components using "shooting" methods rather than to use the above techniques. To do this, we employ a trial-and-error technique of matching the boundary condition at the surface of the outer conductor. Although this approach of solving boundary value problems has been previously used in solving various mechanical and heat transfer problems [7], it has not been used in solving cylindrical waveguide problems.

As an example, we treat the coaxial waveguide system shown in Fig. 1, where there are no azimuthal or axial variations in the permittivity. The radial variation of the dielectric constant in the region between the two conductors is assumed to be describable in terms of an appropriate mathematical function. In this case, Maxwell's curl equations may be expressed by four ordinary first-order differential equations and the boundary conditions can be obtained by setting the tangential electric fields equal to zero at the conducting walls. These equations can be solved by iteration techniques for a given frequency by making sure that the boundary conditions are satisfied at the inner conductor ( $r=a$ ) and by assuming a value for the propagation constant  $\beta$ . Only those values of  $\beta$  that lead to zero tangential electric fields at the outer radius, however, are valid eigenvalues for this system. Consequently, the dispersion curve for a given mode is obtained by systematically choosing values of  $\beta$  for each frequency until the field equations are satisfied in the dielectric region and at both boundaries.

This technique of determining the dispersive properties of the line is essentially a trial-and-error procedure. Nevertheless, it does present a number of advantages for the case of an azimuthally symmetric circular waveguide structure. Since all field components are computed in the determination of the correct  $\beta$  value, these field components are available for printout or display. Also, the ability to select the size of radial increments used in the iteration procedure allows this technique to yield good accuracy for higher order modes and strong radial inhomogeneities of the permittivity.

In Section II, an outline of the theory for rotationally symmetric coaxial waveguides is given. Solutions of the EM fields inside two different radially inhomogeneous coaxial lines are then given for various propagation modes in Section III. Comments are also made regarding the computational time and accuracy of this technique.

## II. THEORY AND SOLUTION METHOD

For harmonic time variation, the electric field  $\vec{E}$  and the magnetic field  $\vec{H}$  in an inhomogeneous dielectric obey Maxwell's two curl equations

$$\nabla \times \vec{E} = -j\omega\mu\vec{H} \quad (1)$$

and

$$\nabla \times \vec{H} = j\omega\epsilon(r)\vec{E}. \quad (2)$$

If the dielectric medium is rotationally symmetric, does not change in the axial direction, and is lossless, the fields vary as  $\exp [j(n\phi - \beta z)]$  (i.e.,  $\beta$  is restricted to real values only). Taking the phase between the various components into account by defining the terms  $H_r = jH_\phi$ ,  $H_\phi = H_\phi$ ,  $H_z = H_z$ ,  $E_r = E_r$ ,  $E_\phi = jE_\phi$ , and  $E_z = jE_z$ , the following set of first-order differential equations are obtained:

$$E_z' = \frac{1}{\omega\epsilon} [\omega^2\mu\epsilon - \beta^2]H_\phi - \frac{\beta n}{\omega r\epsilon} H_z \quad (3)$$

$$E_\phi' = \frac{\beta n}{\omega r\epsilon} H_\phi + \frac{1}{\omega\epsilon} \left[ \frac{n^2}{r^2} - \omega^2\mu\epsilon \right] H_z - \frac{E_\phi}{r} \quad (4)$$

$$H_z' = \frac{1}{\omega\mu} [\omega^2\mu\epsilon - \beta^2]E_\phi - \frac{\beta n}{\omega r\mu} E_z \quad (5)$$

$$H_\phi' = \frac{1}{\omega\mu} \left[ \frac{n^2}{r^2} - \omega^2\mu\epsilon \right] E_z + \frac{\beta n}{\omega r\mu} E_\phi - \frac{H_\phi}{r} \quad (6)$$

$$E_r = \frac{\beta}{\omega\epsilon} H_\phi + \frac{n}{\omega r\epsilon} H_z \quad (7)$$

$$H_r = -\frac{\beta}{\omega\mu} E_\phi - \frac{n}{\omega r\mu} E_z \quad (8)$$

where the prime represents a differentiation with respect to  $r$ . It should be noted that  $H_\phi$ ,  $H_z$ ,  $E_\phi$ , and  $E_z$  can be obtained by the iteration [7] of (3)–(6) if  $E_\phi$  and  $E_z$  are set equal to zero at  $r=a$  and the proper value of  $\beta$  is chosen. The values of  $E_r$  and  $H_r$  can then be obtained by substituting these values into (7) and (8). Furthermore, the  $E$  and  $H$  fields obtained also satisfy Maxwell's divergence equations because those equations follow from taking the divergence of (1) and (2).

It has been shown that transverse electric and transverse magnetic modes can propagate along a transversely inhomogeneous waveguide if the fields do not vary azimuthally [1]. These modes are designated as  $TE_{0m}$  and  $TM_{0m}$  modes, respectively. Other more complicated modes can also propagate in the coaxial waveguide shown in Fig. 1. These modes are called hybrid modes because all of the field components are nonzero. Here they are designated as  $EH_{nm}$  modes, where  $n$  represents the number of angular variations and  $m$  represents the number of radial variations of the field components. Fortunately, all of these modes can be characterized in terms of the magnetic field components at the inner conductor. It can be seen from (3)–(8) that the  $TE_{0m}$  modes have no  $\phi$  component of the magnetic field at  $r=a$ , whereas the  $TM_{0m}$  modes have no  $z$  component of the magnetic field at  $r=a$ . The  $EH_{nm}$  modes, on the other hand, have both components  $H_\phi(a)$  and  $H_z(a)$ , and it is therefore necessary to determine the ratio  $H_\phi(a)/H_z(a)$  in addition to  $\beta$  when computing the fields.

The procedure used to obtain the dispersion curve for each mode can be described as follows.

1) The permittivity of the radially inhomogeneous dielectric is represented by an appropriate function in the region between the two conductors.

2) The ratio  $H_\phi(a)/H_z(a)$  ( $H_\phi(a)/H_z(a) = 0$  for  $TE_{0m}$  modes, etc.) is chosen and (3)–(8) are iterated from  $r=a$  to  $r=b$  for various  $\beta$  values ( $\omega$  is held constant) until the boundary conditions at the outer conductor are met.

3) If the boundary conditions at  $r=b$  cannot be met (for hybrid modes), step 2) is repeated using a different value of  $H_\phi(a)/H_z(a)$  until the boundary conditions are satisfied.

4) The dispersion curve is then obtained by repeating steps 2) and 3) for the frequencies  $\omega$ ,  $\omega + \Delta\omega$ ,  $\dots$ ,  $\omega + k\Delta\omega$ ,  $\dots$ ,  $\omega + n\Delta\omega$  (where  $\Delta\omega$  is the frequency interval between points on the dispersion curve).

In obtaining the dispersion curve, the computer algorithm systematically searches for those values of  $\beta$  that approximate the boundary conditions at each frequency. In each case, the fields are computed out to  $r=b$ , and the magnitudes of  $E_\phi(b)$  and  $E_z(b)$  are checked to de-

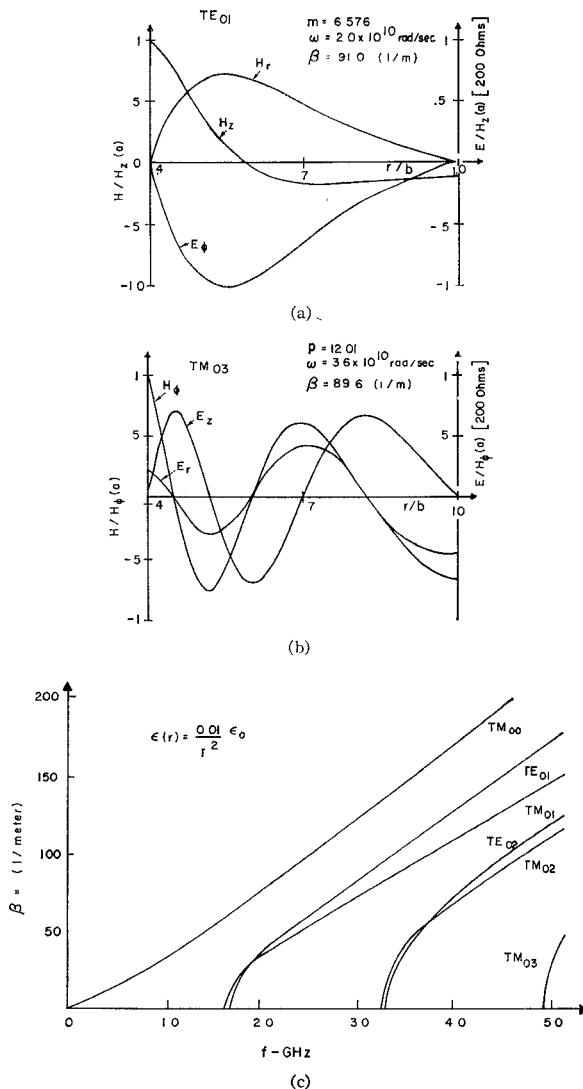


Fig. 2. Typical EM field distributions for permittivity proportional to  $r^{-2}$ . (a) TE<sub>01</sub> mode. (b) TM<sub>03</sub> mode. (c) Dispersion curves.

termine if these field components fall within some small interval around zero. If they do not, the search procedure is continued until  $E_\phi(b)$  and  $E_z(b)$  approximate the boundary conditions within the pre-determined error.

The fields obtained by the above procedure represent valid mode solutions because they satisfy Maxwell's equations throughout the region, including the boundaries. In the following section, examples are given that indicate the usefulness of the above approach.

### III. EXAMPLES

In order to illustrate the usefulness of the direct computational technique discussed previously, we present two examples in this section. The first example considered is the radially inhomogeneous coaxial transmission line treated analytically by Ah Sam and Klinger [1]. The second example is that of a coaxial transmission line in which a gaseous discharge occupies the region between the inner and outer conductor.

#### A. Example I— $\epsilon_0 l/r^2$ Dielectric Inhomogeneity

As a first example, we treat the coaxial line having a radial inhomogeneity in the permittivity given by  $\epsilon_0 l/r^2$  ( $l$ =constant). This example is particularly illustrative because it is one of the very few examples that has an analytical solution.

The field components for the TE<sub>01</sub> mode and the TM<sub>03</sub> mode are shown in Fig. 2(a) and (b) for the case where  $l=0.01$  m<sup>2</sup>,  $a=0.04$  m, and  $b=0.1$  m. Both of these solutions were obtained in less than 10 s

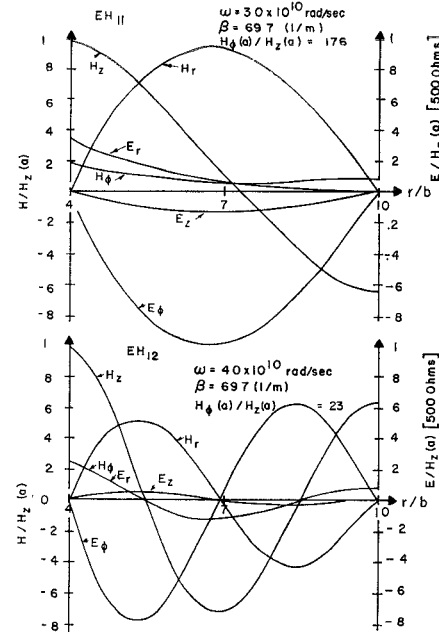


Fig. 3. Typical hybrid field distribution for permittivity of Example 2. (a) EH<sub>11</sub> mode. (b) EH<sub>12</sub> mode.

from a CDC 3600 computer using 60 iterations, and the magnitude of  $E_\phi(b)$  and  $E_z(b)$  was less than  $10^{-5}$  times the peak value of  $E_\phi(r)$  and  $E_z(r)$  in both cases.

The dispersion curves for various TE<sub>0m</sub> and TM<sub>0m</sub> modes have been determined for this example and are shown in Fig. 2(c). It is seen that the TM<sub>00</sub> mode is the dominant waveguide mode for this structure. As a check, the dispersion curves for the TE modes were compared with the analytical results of Ah Sam and Klinger [1]. These modes were seen to satisfy the dispersion relationship

$$\frac{I_m(\beta a)}{K_m(\beta b)} = \frac{I_m(\beta b)}{K_m(\beta a)}$$

where  $I_m(x)$  and  $K_m(x)$  are modified Bessel functions of the first and second kind. Hybrid modes can also be observed in the frequency range shown corresponding to each set of TE<sub>0n</sub>-TM<sub>0n</sub> modes. However, we will delay further discussion of these modes to the next example.

#### B. Example II—The Radial Coaxial Gas Discharge

For a second example, we choose to deal with the experimental system of McIntosh and Andrews [8] that includes a coaxial transmission line in which the dielectric medium between the two conductors is inhomogeneous, owing to a low-pressure gaseous discharge. Electron number density and temperature measurements have been made for this system using a Langmuir probe and a microwave interferometer with the result that the permittivity has been determined as a function of radius. The dependence of  $\epsilon$  on frequency is due to the intrinsic dispersion of the ionized medium. We are able to approximate the permittivity with a Gaussian distribution such that

$$\epsilon(r) = \epsilon_0 \left[ 1 - \frac{(B^2 \exp[-(r - r_0)^2/2\sigma^2] + A^2)}{\omega^2} \right]$$

where  $B$  and  $A$  are two constants such that  $B+A=\Pi$  (the peak plasma frequency at  $r=r_0$ ),  $\omega$  is the frequency of the EM wave, and  $\sigma$  is the standard deviation of the permittivity profile. In the example treated here,  $A=9.75 \times 10^9$  rad/s,  $B=11.7 \times 10^9$  rad/s,  $\Pi=15.25 \times 10^9$  rad/s, and  $\sigma=0.7917$  m<sup>2</sup>.

The fields of various modes are shown in Figs. 3 and 4(a) and (b). The lowest order mode is the TM<sub>00</sub> mode, which is shown in Fig. 4(a). This mode represents a perturbation of the TEM mode, which exists in a homogeneous coaxial line. Thus the field components  $E_z$  lessen as the frequency increases (and the dielectric inhomogeneity decreases). The TM<sub>01</sub> mode shown in Fig. 4(b) is plotted with those

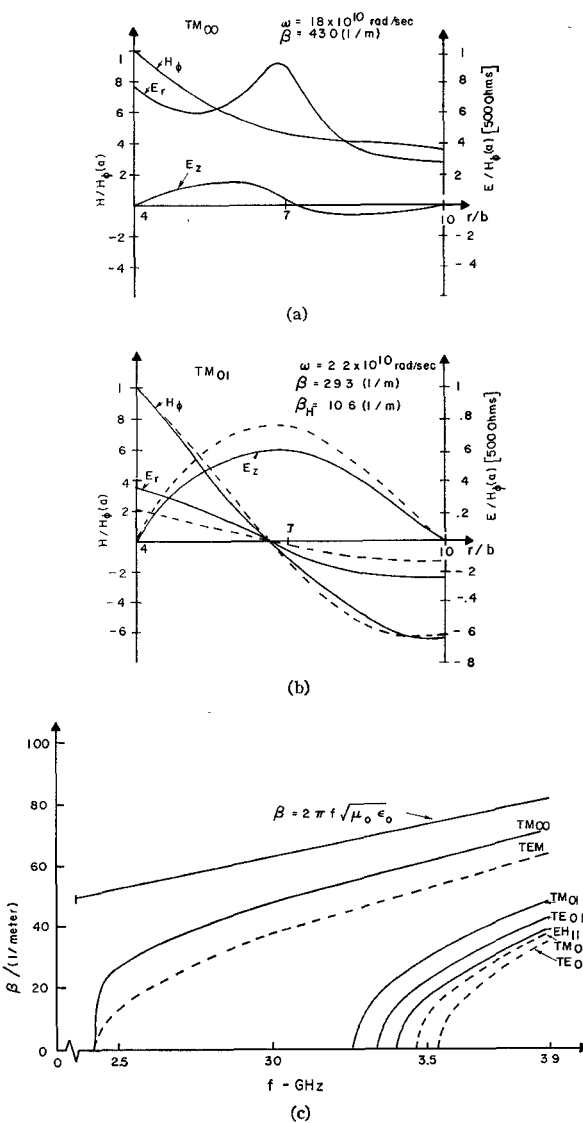


Fig. 4. Typical EM field distributions for permittivity of Example 2. (a)  $TM_{00}$  mode (fundamental mode). (b)  $TM_{01}$  mode (dashed curves represent field distributions in a coaxial line filled uniformly with a plasma having  $\Pi = 15.25 \times 10^9$  rad/s;  $\beta_H$  is the propagation constant for the uniform case.) (c) Dispersion curves for permittivity of Example 2 and for a coaxial waveguide filled with a homogeneous plasma.

fields that would exist in a coaxial line, if the electron plasma frequency were uniform and equal to  $\Pi$ . It is seen that the alterations in the field components for the higher order modes are smaller because the permittivity inhomogeneity is not appreciable in the frequency range where the higher modes propagate.

The field variations for the first two hybrid modes are shown in Fig. 3 when  $\omega/\Pi = 2.29$ . These fields were obtained by systematically trying different ratios of  $H_\phi(a)/H_s(a)$  in the search procedure outlined in Section II. In the case of the  $EH_{11}$  mode, this ratio is approximately  $H_\phi(a)/H_s(a) = 0.176$ , and for the  $EH_{12}$  mode,  $H_\phi(a)/H_s(a) = 0.230$ . The cutoff frequencies of higher hybrid modes are sufficiently great that the permittivity of the medium is essentially that of free space in the frequency range where these modes propagate. Consequently, these modes are approximately linear combinations of  $TE_{mn}$  and  $TM_{mn}$  modes that can propagate in a homogeneous coaxial line.

Dispersion curves (solid lines) for the modes discussed above are seen in Fig. 4(c) for the example treated. Dispersion plots (dotted lines) are also given for those modes that would propagate along a homogeneously filled plasma coaxial line. Although the cutoff frequency of the fundamental ( $TM_{00}$ ) mode occurs at the same frequency ( $\omega = \Pi$ ) as the cutoff frequency of the homogeneous line, the

cutoff appears to be much sharper. The cutoff frequencies for the higher order modes, on the other hand, differ significantly. For these modes, the cutoff frequency obtained by considering the dielectric inhomogeneity is lower than that of coaxial modes in a homogeneous line having a dielectric constant  $\epsilon = \epsilon_0(1 - \Pi^2/\omega^2)$ . The cutoff frequencies of these inhomogeneous modes correspond more closely to the cutoff frequency of modes in a uniform coaxial line where the dielectric constant is the average value

$$\langle \epsilon \rangle = \left[ \int_a^b \epsilon(r) r dr \right] / (b - a).$$

### C. Discussion

The speed and accuracy with which the field calculations were carried out indicate that the procedure employed is practical for arbitrary radial inhomogeneities of the electrical properties of the medium. In every instance, the computing time required to calculate the field solution at each frequency for the above examples was less than 10 s. The accuracy of these solutions was checked by substituting the numerical solutions obtained into Maxwell's divergence equations, which for our system can be written as

$$H_r' = -\frac{n}{r} H_\phi + \beta H_z - \frac{H_r}{r} \quad (10)$$

and

$$E_r' = \frac{n E_\phi}{r} - \beta E_z - \left[ \frac{1}{r} - \frac{\epsilon'}{\epsilon} \right] E_r. \quad (11)$$

In every case, the values of  $H_r'$  and  $E_r'$  obtained from (10) and (11) were within 1 percent of the values calculated in the main routine. The accuracy of the procedure was also checked by comparing numerical solutions with known analytical solutions of the higher order modes in a homogeneous coaxial line. The computed cutoff frequencies and dispersion curves were within 1 percent of the analytically determined values below the  $TE_{0,30}$  coaxial waveguide mode.

### REFERENCES

- [1] E. Ah Sam and V. Klinger, "Propagation in cylindrical waveguide containing inhomogeneous dielectric," *IEEE Trans. Microwave Theory Tech. (Corresp.)*, vol. MTT-15, pp. 60-61, Jan. 1967.
- [2] R. Yamada and K. Watanabe, "Propagation in cylindrical waveguide containing inhomogeneous dielectric," *IEEE Trans. Microwave Theory Tech. (Corresp.)*, vol. MTT-13, pp. 716-717, Sept. 1965.
- [3] G. Goubau, "Surface waves and their application to transmission lines," *J. Appl. Phys.*, vol. 21, pp. 1119-1128, Nov. 1950.
- [4] J. L. Shohet and A. J. Hatch, "Eigenvalues of a microwave cavity filled with a plasma of variable radial density," *J. Appl. Phys.*, vol. 41, pp. 2610-2618, May 1970.
- [5] V. N. Krepak and I. P. Yakimenko, "E-waves in circular waveguide with inhomogeneous plasma," *Radio Eng. Electron. Phys.*, vol. 14, no. 3, pp. 364-369, Mar. 1969.
- [6] W. J. English, "Vector variational solutions of inhomogeneously loaded cylindrical waveguide structures," *IEEE Trans. Microwave Theory Tech.*, vol. MTT-19, pp. 9-18, Jan. 1971.
- [7] B. Carnahan, H. A. Luther, and J. O. Wilkes, *Applied Numerical Methods*. New York: Wiley, 1969, pp. 405-406.
- [8] R. E. McIntosh and R. G. Andrews, "Dispersion of transient electromagnetic signals propagating along a coaxial gas discharge," *J. Appl. Phys.*, vol. 42, no. 5, pp. 1857-1862, Apr. 1971.

### A Quick Accurate Method to Measure the Dielectric Constant of Microwave Integrated-Circuit Substrates

JOHN Q. HOWELL

**Abstract**—A technique is described that makes possible the accurate measurement of the dielectric constant of microwave integrated-circuit substrates. The substrate is metallized on all sides, hence forming a tiny resonant cavity, and the resonant frequencies are determined either from transmission or reflection. The dielectric constant is then calculated to an accuracy of better than 1 percent.